Petrick, C., Matthes, K., Dobslaw, H., Thomas, M. (2012): Impact of the solar cycle and the QBO on the atmosphere and the ocean. - Journal of Geophysical Research, 117, D17

DOI: 10.1029/2011JD017390

Impact of the solar cycle and the QBO on the atmosphere and the ocean

C. Petrick,[1,2] K. Matthes,[1,2,3] H. Dobslaw,[1] and M. Thomas[1,3]

Received 22 December 2011; revised 2 July 2012; accepted 26 July 2012; published 7 September 2012.

[1] The solar cycle and the Quasi-Biennial Oscillation are two major components of natural climate variability. Their direct and indirect influences in the stratosphere and troposphere are subject of a number of studies. The so-called "top-down" mechanism describes how solar UV changes can lead to a significant enhancement of the small initial signal and corresponding changes in stratospheric dynamics. How the signal then propagates to the surface is still under investigation. We continue the "top-down" analysis further down to the ocean and show the dynamical ocean response with respect to the solar cycle and the QBO. For this we use two 110-year chemistry climate model experiments from NCAR's Whole Atmosphere Community Climate Model (WACCM), one with a time varying solar cycle only and one with an additionally nudged QBO, to force an ocean general circulation model, GFZ's Ocean Model for Circulation and Tides (OMCT). We find a significant ocean response to the solar cycle only in combination with a prescribed QBO. Especially in the Southern Hemisphere we find the tendency to positive Southern Annular Mode (SAM) like pattern in the surface pressure and associated wind anomalies during solar maximum conditions. These atmospheric anomalies propagate into the ocean and induce deviations in ocean currents down into deeper layers, inducing an integrated sea surface height signal. Finally, limitations of this study are discussed and it is concluded that comprehensive climate model studies require a middle atmosphere as well as a coupled ocean to investigate and understand natural climate variability.

Citation: Petrick, C., K. Matthes, H. Dobslaw, and M. Thomas (2012), Impact of the solar cycle and the QBO on the atmosphere and the ocean, *J. Geophys. Res.*, *117*, D17111, doi:10.1029/2011JD017390.

1. Introduction

[2] One of the most important sources of natural climate variability is provided by the Sun on different timescales, and its climate influence is under continued discussion. Recently, *Gray et al.* [2010] provided a comprehensive review of solar influences on the climate system. One complication of the solar cycle influence is the (possible non-linear) interaction with the Quasi-Biennial Oscillation (QBO) of equatorial stratospheric winds first noted by *Labitzke* [1987] and *Labitzke and Loon* [1988]. *Kodera and Kuroda* [2002] introduced the so-called "top-down" mechanism for the stratosphere. This mechanism describes how relatively small UV variations with the 11-year solar cycle in the tropical upper stratosphere can lead to a significantly enhanced dynamical response throughout the stratosphere. Changes in middle atmosphere heating and therefore in ozone production and loss induce changes in the meridional temperature gradients, which in turn alter the propagation properties for planetary waves and lead to circulation changes. However, the effects of the solar cycle are not confined to the stratosphere. Further down, e.g., *White et al.* [1997] noted a small decadal to interdecadal solar cycle effect in globally averaged Sea Surface Temperatures (SSTs). Later, *Roy and Haigh* [2010] found in agreement with other authors a significant solar cycle response during boreal winter in the surface pressure (i.e., a weakening of the Aleutian Low and a northward shift of the Hawaiian High during solar maximum (S_{max})). On the Southern Hemisphere (SH), *van Loon and Meehl* [2011] found significant positive Sea Level Pressure (SLP) anomalies in the south east Pacific during S_{max} conditions.

[3] Most modeling studies have difficulties to reproduce the pattern and magnitude of the observed climate system response to the solar cycle. *Meehl et al.* [2009] suggested that in addition to the "top-down" mechanism a so-called "bottom-up" mechanism takes place in which the ocean feedback amplifies the solar cycle effect. Taking into account the middle atmosphere and the ocean improves the amplitude of the modeling results. The importance of other sources of natural variability (e.g., the QBO) on the climate system's

[1]Helmholtz Centre Potsdam, German Research Centre for Geosciences, Potsdam, Germany.
[2]Now at GEOMAR, Helmholtz Centre for Ocean Research Kiel, Kiel, Germany.
[3]Institut für Meteorologie, Freie Universität Berlin, Berlin, Germany.

Corresponding author: C. Petrick, GEOMAR, Helmholtz Centre for Ocean Research Kiel, DE-24148 Kiel, Germany. (cpetrick@geomar.de)

0148-0227/12/2011JD017390

Table 1. Description of Atmospheric and Oceanic Experiments Depending on Their Forcing

Forcing	Atmosphere	Ocean
Solar Cycle only	A^{SC}	O^{SC}
Solar Cycle and QBO	A^{SC}_{QBO}	O^{SC}_{QBO}

solar cycle response is for example discussed in a model study by *Matthes et al.* [2010].

[4] To shed more light on the response of the ocean to the "top-down" mechanism, we extend the "top-down" investigation in the atmosphere by adding a dynamic ocean model. Therefore we use two 110-year model experiments of NCAR's Whole Atmosphere Community Climate Model (WACCM), a fully coupled chemistry-climate model (CCM) [*Garcia et al.*, 2007], to force GFZ's Ocean Model for Circulation and Tides (OMCT) [*Thomas et al.*, 2001], an Ocean General Circulation Model (OGCM). Both atmospheric experiments include a time varying solar forcing, but only one includes a (prescribed) QBO (K. Matthes et al., Role of the QBO in modulating the influence of the 11-year solar cycle on the atmosphere using variable forcings, submitted to *Journal of Geophysical Research*, 2012JD017764, 2012). In order to isolate the "top-down" effect, our atmospheric simulations used climatological SSTs. The modeled atmospheric data are then used to force the ocean model. This contrasts the experimental design of *Meehl et al.* [2009], who compare three different model settings: WACCM standalone (for analyzing the top-down mechanism); WACCM coupled to an ocean (combined top-down and bottom up); and CAM coupled to an ocean (bottom-up). All three model studies do not include a QBO. The present study instead focuses solely on the signal that propagates from the stratosphere through the troposphere into the ocean, excluding all ocean feedbacks, i.e. "bottom-up" mechanism. The goal is to investigate whether prescribed stratospheric winds, i.e. the QBO, significantly affect not only the stratospheric, but also the tropospheric and the oceanic response to the solar cycle.

[5] This paper is structured as follows: the description of the dynamic ocean model as well as the experimental design and the analysis methods, are given in section 2. Section 3 and 4 describe the results of the model experiments, in particular the impact of the QBO and the solar cycle on the atmosphere and their subsequent effects on ocean dynamics. Sections 5 and 6 summarize and conclude the results.

2. Model Description and Experimental Design

2.1. Model Description

[6] The experiments were carried out with the Ocean Model for Circulation and Tides (OMCT) [*Thomas et al.*, 2001] which is based on the Hamburg Ocean Primitive Equation model (HOPE) [*Wolff et al.*, 1996; *Drijfhout et al.*, 1996] but additionally includes an ephemeral tidal model, which is disabled in our experiment. The OMCT solves the nonlinear momentum equations, applying the hydrostatic and Boussinesq approximations. It also satisfies the continuity equations and conservation equations for heat and salt. The horizontal velocity components, water elevation, potential temperature and salinity distribution are prognostically calculated variables. The vertical velocity component is calculated diagnostically using the continuity equation. Ice-thickness, compactness, and drift are predicted with the included prognostic thermodynamic sea-ice model. The OMCT has a horizontal resolution of $1.875° \times 1.875°$ and 13 vertical layers. The model time step is 30 min. Atmospheric meridional and zonal wind stress, surface pressure, 2 m temperature and freshwater fluxes are used to force the model. The OMCT is generally used at GFZ to de-alias GRACE satellite data [*Flechtner*, 2007]. Recently, Dobslaw et al. [2010] used ERA-reanalysis data to force the OMCT and a continental hydrosphere model to investigate the contributions of the Earth subsystems (atmosphere, ocean, hydrosphere) to Earth rotation, i.e. polar motion.

[7] We carried out two 110-year simulations with the OMCT (see Table 1). The atmospheric forcing for these long-term OMCT runs came from two 110-year simulations of NCAR's Whole Atmosphere Community Climate Model (WACCM), version 3.19, as described by Matthes et al. (submitted manuscript, 2012). WACCM is a fully interactive Chemistry-Climate Model (CCM) resolving the troposphere, the stratosphere, and the mesosphere up to the thermosphere [5.1×10^{-6} hPa ($\sim$140 km)] [*Garcia et al.*, 2007]. WACCM3 is an expanded version of the Community Atmospheric Model, Version 3 (CAM3) and includes all of the physical parametrization of CAM3 [*Collins et al.*, 2006]. The detailed neutral chemistry model for the middle atmosphere is based on the Model for Ozone and Related Chemical Tracers, Version 3 (MOZART3) and accounts for radiatively active gases affecting heating and cooling rates and hence dynamics [*Kinnison*, 2007]. The horizontal resolution is $1.9° \times 2.5°$ and 66 vertical levels are included. Because WACCM is not able to generate an internal QBO, modeled tropical stratospheric zonal winds are relaxed toward observations in the equatorial band from 22°N to 22°S [*Matthes et al.*, 2010].

2.2. Experimental Design

[8] Two transient 110-year simulations of WACCM were carried out under natural forcings only, one solely with the 11-year solar cycle, i.e. a varying solar spectral irradiance (A^{SC}), and the other one with both a solar cycle and a QBO (A^{SC}_{QBO}). As a proxy for the solar cycle irradiance, we use the f10.7 cm solar radio flux. Geomagnetic activity is accounted for by the kp-index. All other natural and anthropogenic forcings were held constant at 1995 conditions (i.e. climatological monthly varying SSTs, Green House Gases (GHGs), and Ozone Depleting Substances (ODS)). No volcanic effects are included. Since we do not have solar cycle and QBO observations for 110 years, the observed f10.7 cm solar radio flux, the kp-index as well as the equatorial winds in the tropical lower stratosphere from 1953 to 2004 were extended with two repetitions of the years from 1962 to 2004 (Matthes et al., submitted manuscript, 2012). We choose the year 1962 because the solar cycle and the QBO show similar phases as in 2004, allowing a smooth continuation. These two atmospheric simulations were used to force the dynamic ocean model in order to study the oceanic sensitivity to the prescribed natural forcings, yielding experiments O^{SC} and O^{SC}_{QBO}. Note that in the experiments presented here, no freshwater fluxes were accounted for.

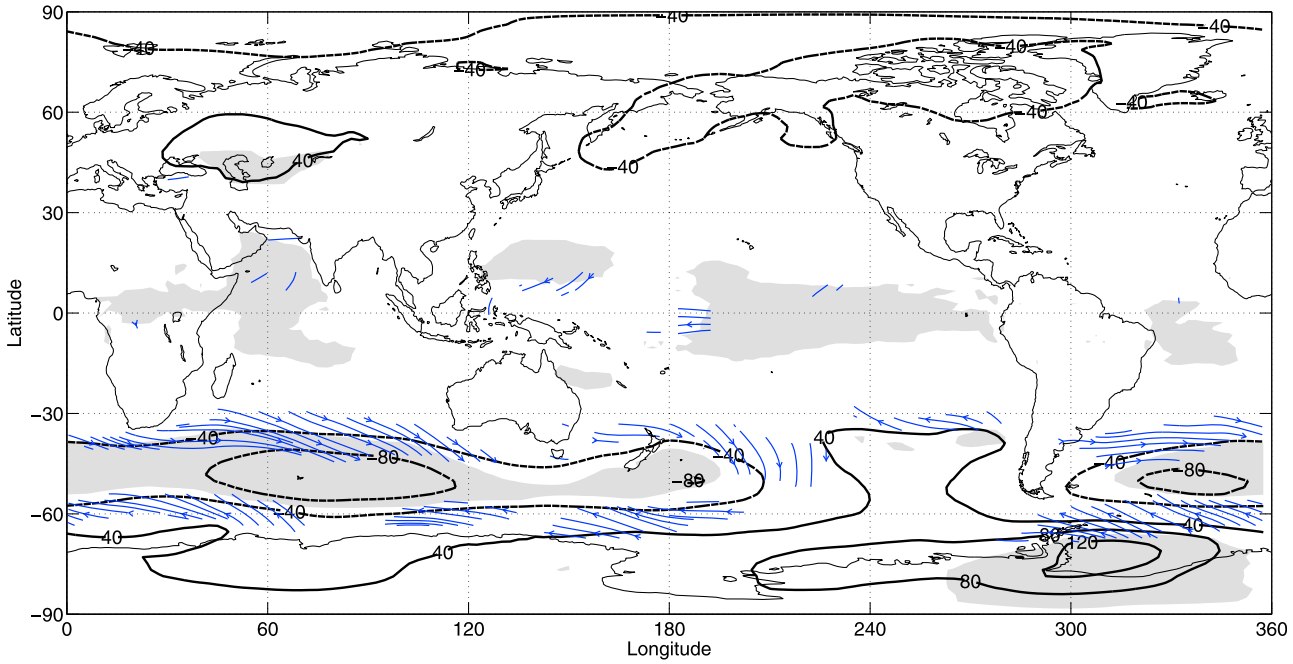

Figure 1. Composite mean difference between $QBO_{west} - QBO_{east}$ of surface pressure in Pa. Shaded regions denote 99% significance. Arrows represent 99% significant surface wind anomalies. The significant surface wind anomalies in the southern hemisphere reach an amplitude of $0.75\frac{m}{s}$ in the south Atlantic and $0.5 - 0.6\frac{m}{s}$ in the south Pacific and Indian ocean.

[9] *Rind et al.* [2008] found a partly statistically significant solar cycle related precipitation reduction near and south of the equator of about 1 millimeter per day for August and an increase in precipitation north of the equator especially above south Asia with a similar amplitude. The precipitation effect is spatially localized and variable over the year. *Huang and Mehta* [2005] indicated that precipitation changes of about 1.5 m/yr on interannual timescales have the potential to influence the baroclinic circulation of an ocean. However, the OMCT is not forced by precipitation itself, but by the net freshwater flux (precipitation minus evaporation). Based on this and the results from *Rind et al.* [2008] and *Huang and Mehta* [2005] we expect solar cycle related precipitation changes to have only minor effects on our modeling results, especially since we investigate multidecadal monthly mean results. The way our heat flux is parameterized may have the potential to alter clouds and thus the incoming short wave radiation, which in turn might influence local heating.

2.3. Methods and Data

[10] We analyze monthly mean model data, which are deseasonalized by subtracting the long-term monthly means from each month of the time series. We then use the composite mean differences (CMD) between the solar maximum ($S_{\max}$) minus the solar minimum ($S_{\min}$) months to visualize the influences of the solar cycle. Here solar maximum and minimum months are defined according to Matthes et al. (submitted manuscript, 2012), with $S_{\max}$: f10.7 cm solar radio flux > 150 solar flux units ($10^{-22}\frac{W}{m^2 Hz}$, hereafter sfu) and $S_{\min}$: f10.7 cm solar radio flux < 90 sfu. The composites include 348 $S_{\max}$ and 391 $S_{\min}$ months. For additional confirmation of our results we computed the correlation between the f10.7 and the model output. The difference between the correlation and the CMD results in terms of significance patterns is marginal; the correlation of the resulting spatial patterns of both methods exceeds 0.9. The 99% statistical significance is determined with a Student's t-test, taking into account the auto-correlation by reducing the degrees of freedom accordingly. The significance patterns as well as the anomalies are also verified by bootstrap analysis, using 1000 samples. All three methods yield very similar signals and significances.

3. QBO Footprint and Solar Signal in the Atmosphere

[11] In order to investigate the response of the atmosphere and the ocean to varying natural forcings such as the QBO and the solar cycle, we start analyzing the effect of the QBO, using the atmospheric A^{SC}_{QBO} and the corresponding oceanic O^{SC}_{QBO} experiment. Afterward, we compare the solar cycle response of this realization to the solar cycle only (A^{SC}) experiment. Figure 1 shows the CMD in atmospheric surface pressure where the QBO signal has been lagged by 4 months. A lag of 4 months yields the most significant signal and agrees with *Marsh and Garcia* [2007], who found that the correlation between 52 hPa temperature and ozone and the surface NINO3.4 index in WACCM peaks at a lag of 4–5 months. They also indicate that this is the model-related coupling time between the stratosphere and the surface troposphere.

[12] In Figure 1 we find significant negative pressure anomalies in the SH, between $30°S$ and $60°S$, peaking in the south Atlantic and south Indian Ocean with a maximum amplitude of 100 Pa. In the south polar region we find positive pressure anomalies for $QBO_{west} - QBO_{east}$ of more

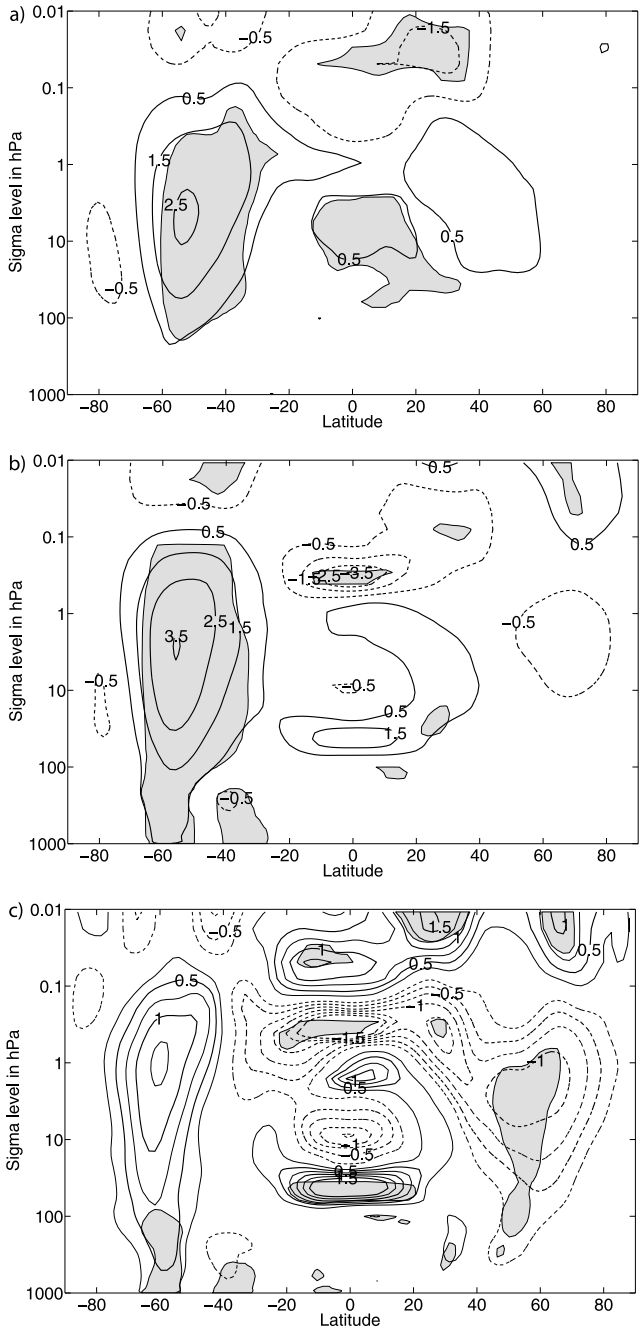

Figure 2. Annual mean composite mean difference between $S_{\max} - S_{\min}$ of zonal mean zonal wind for (a) A^{SC}, (b) A^{SC}_{QBO}, and (c) $A^{SC}_{QBO} - A^{SC}$. Shaded regions denote 99% significance. Contour lines denote anomalies in $\frac{m}{s}$, negative values are dashed.

than 120 Pa, significant mainly in the vicinity of the Weddel Sea. The pressure anomalies in the SH show a negative SAM-like pattern and are associated with significant wind anomalies, represented by blue streamlines. The wind anomalies shown are significant at the 99% level and have an amplitude of about $0.7\frac{m}{s}$. However, these significant atmospheric surface anomalies do not propagate into the ocean (not shown), because the signal amplitude is very fast and its amplitude is too weak.

[13] We also find significant pressure anomalies in the equatorial Pacific, Indian and Atlantic oceans. However, these signals are very weak, with a maximum amplitude of about 10 Pa. Because the variability of the deseasonalized equatorial surface data is low, small differences between the QBO phases are significant. In contrast the Northern Hemisphere (NH) shows stronger negative anomalies of up to 50 Pa, which are, however, not significant due to the high variability of the signal here.

[14] Summarizing, we find a significant atmospheric surface signal for the lagged $QBO_{west} - QBO_{east}$ CMD, which do not propagate into the ocean. We further concentrate on the solar cycle response of our modeled atmospheres for both the solar cycle only (A^{SC}, O^{SC}) and the solar cycle plus QBO (A^{SC}_{QBO}, O^{SC}_{QBO}) experiments.

3.1. Solar Signal in the Zonal Mean Zonal Wind Considering the QBO

[15] The CMD of the atmospheric zonal mean zonal wind with the solar cycle is shown in Figure 2a for the WACCM simulation with solar cycle only (A^{SC}) and Figure 2b for the WACCM simulation with solar cycle and nudged QBO (A^{SC}_{QBO}). Both figures differ especially in the SH troposphere. The A^{SC} run shows significant positive anomalies mainly above 100 hPa, peaking in southern midlatitudes between 30° and 60°S and at the equatorial regions at 10 hPa. Negative values are present in the equatorial mesosphere above 0.1 hPa (Figure 2a).

[16] Prescribing the QBO leads to a significant strengthening of the atmospheric solar cycle response especially on the SH troposphere (Figure 2b). Now we find stronger positive anomalies, reaching from the lower mesosphere / upper stratosphere down to the surface between 50° and 60°S. The amplitude of the positive anomalies increases by about $1\frac{m}{s}$ to a maximum of about $3.5\frac{m}{s}$. Additionally significant negative values are present in the troposphere between 25° and 40°S. The significant positive anomalies in the equatorial stratosphere vanishes because the QBO nudging zone is located here. One can see a QBO signature in the equatorial stratosphere, which indicates that the solar cycle composite does not filter the QBO signal entirely (see auxiliary material Figure S3 for the QBO composite).[1] The reason why we see a QBO footprint in the solar cycle composite is related to the fact, that during $S_{\max}$ conditions (total of 348 months) there are 144 QBO_{west} and 124 QBO_{east} months, or in other words a slight tendency toward the QBO_{west} phase. During $S_{\min}$ conditions (total of 391 months) we find 143 QBO_{west} and 156 QBO_{east} months, indicating a slight tendency toward the QBO_{east} phase. Therefore, the $S_{\max} - S_{\min}$ composite shows slight $QBO_{west} - QBO_{east}$ features. This does not indicate a phenomenological connection between the solar cycle and the QBO, since both time series are prescribed in this modeling study.

[17] The weak positive anomalies in the northern stratosphere found for the A^{SC} experiment (Figure 2a), turn into weak negative anomalies when prescribing the QBO (Figure 2b); both are not significant. Comparing both solar cycle responses (Figure 2c: $A^{SC}_{QBO} - A^{SC}$) with each other

[1] Auxiliary materials are available in the HTML. doi:10.1029/2011JD017390.

reveals that the increase of the zonal mean zonal wind in the SH is only significant for the troposphere, but not for the stratosphere. This means that an increase of zonal mean zonal wind of about $1\frac{m}{s}$ at the height of 1 hPa is not significant, while the increase of $0.4\frac{m}{s}$ in the troposphere is significant for both cases: $S_{\max} - S_{\min}$ (Figure 2b) and for $A^{SC}_{QBO} - A^{SC}$ (Figure 2c). Since we have about 10 solar cycles in the 110 years of model output, the signal-to-noise ratio could be further improved by continuing the experiment. This may increase the significance of certain patterns, for example the strengthening of the southern stratospheric jet.

[18] The annual mean zonal mean zonal wind results of experiment A^{SC}_{QBO} (Figure 2b) compare well to the analysis of *Kuroda and Kodera* [2005], who found similar patterns in ERA40 reanalysis data from October through December (OND). These months dominate the annual mean response of the SH (shown in Figure 2). *Thompson and Wallace* [2000] found the SAM coupled with the stratospheric circulation during these months. Our A^{SC}_{QBO} experiment also shows the strongest stratosphere-troposphere coupling during OND, whereas the coupling in the A_{SC} run is weaker. In the auxiliary material (Figures S1 and S2) we provide OND zonal mean zonal wind for the A^{SC} and A^{SC}_{QBO} experiment. This indicates that prescribing the QBO improves the atmospheric solar cycle response compared to observations, as the experiment without QBO does not show these features.

[19] On the NH both experiments (A^{SC}_{QBO}, A^{SC}) show no significant solar cycle response. The NH experiences more interannual variability possibly overwhelming a solar cycle response. Greater land-sea contrast in the NH causes more planetary wave activity which disturbs the polar vortex. Similarly, *Kodera and Kuroda* [2002] found the interannual polar night jet variability substantially larger in the NH compared to the SH. According to the Holton-Tan effect [*Holton and Tan*, 1980, 1982] the NH is more variable during QBO_{east} phase because planetary waves are reflected poleward causing more disturbance in the extratropical stratosphere. In the A^{SC} experiment with no prescribed QBO, we find climatological easterly winds in the equatorial stratosphere. These easterly winds tend to reflect the planetary waves which means a constantly more disturbed polar vortex. Thus we would expect a more variable extratropical stratosphere and hence a smaller and less significant solar cycle response. In fact the A^{SC} experiment shows a weaker zonal mean zonal wind signal in the mid to high latitude troposphere compared to the A^{SC}_{QBO}.

[20] To summarize, we find a significant dynamic response of the atmosphere to the solar cycle, which only propagates to the surface on the southern hemisphere if the QBO is prescribed. Here we would like to mention, that any computed solar response depends on the applied analysis. In order for our results to be better comparable to other studies, we provide various figures in the auxiliary material. The next questions are: How does the atmospheric reaction to the solar cycle looks like at the Earth's surface? And, does this dynamic atmospheric surface state translates into an oceanic response?

3.2. Solar Signal at the Surface Atmosphere Considering the QBO

[21] As shown in Figure 2b, nudging QBO winds in the stratosphere influences the zonal mean zonal winds from the stratosphere down to the surface, especially in the SH. The corresponding surface pressure anomalies as well as significant surface wind vectors are shown in Figure 3b. Here, the surface pressure anomalies show a positive SAM-like pattern, including negative south-polar anomalies and positive annular anomalies in southern midlatitudes, with an amplitude of up to ± 1.3 hPa, which is between 20% and 35% of the local standard deviation of the deseasonalized monthly mean data. The most pronounced and significant anomalies in midlatitudes appear in the southern Indian (around 90°E) and in the southern Pacific Ocean (around 150°W). The two positive pressure anomalies correspond to anticyclonic, counterclockwise winds, whereas the large polar pressure low induces cyclonic winds at high southern latitudes (south of 60°S). The wind anomalies are between $0.5\frac{m}{s}$ and $0.9\frac{m}{s}$ (i.e. 20% to 30% of the local standard deviation), with the maximum located around 60°S. As already stated above, the spatial pattern of the composite mean difference and the correlations, as well as their spatial significance, are very similar.

[22] The solar cycle only experiment (A^{SC}) differs significantly from the experiment with solar cycle and QBO (A^{SC}_{QBO}): The surface pressure anomalies for $S_{\max}$ minus $S_{\min}$ (Figure 3a) are generally smaller and less significant than when the QBO is included (Figure 3b). Instead of the strong SAM-like pattern as seen in the A^{SC}_{QBO} experiments, significant positive anomalies appear south west of Australia as well as in the subtropical south Atlantic and Pacific. Stronger but not significant negative anomalies occur between South America and the Antarctic and over Siberia. The smaller amplitude and the more localized spatial pattern (compared to A^{SC}_{QBO}, Figure 3b) suggest a weaker atmospheric impact on the ocean by the atmosphere when the solar cycle is the only source of natural variability.

[23] *Roy and Haigh* [2010] analyzed 150 years of DJF SLP from the Hadley Centre HadSLP2 data set and found a comparable solar cycle footprint to our A^{SC}_{QBO} experiment in the SH. They also found negative pressure anomalies at the south pole, while the southern midlatitudes show positive anomalies. Their DJF signal was not significant, but compares well in shape to our non-significant DJF signal in A^{SC}_{QBO} experiment (see auxiliary material Figure S4). For the annual mean we find weaker but significant amplitudes (Figure 3b) compared to DJF from *Roy and Haigh* [2010]. The equatorial regions as well as the NH show substantial differences: *Roy and Haigh* [2010] found for DJF a northward shift of the Hawaiian High and a weakening of the Aleutian Low, the latter is in agreement with *van Loon and Meehl* [2011]. In contrast to these observational studies, our model simulations do not show significant signals in the NH, neither for DJF nor for the whole time series. We speculate that the reasons for this dissonance relate mainly to two facts: (1) an incorrect modeling of the atmospheric planetary waves, especially important on the NH; and (2) our atmospheric experiments are forced with climatological SSTs, omitting any ocean feedback and interannual variability, e.g. ENSO. We therefore investigate a pure and idealized "top-down" solar cycle response of the atmosphere and the ocean. The latter indicates the importance of atmosphere-ocean coupling. In the following we exemplarily show, how changes

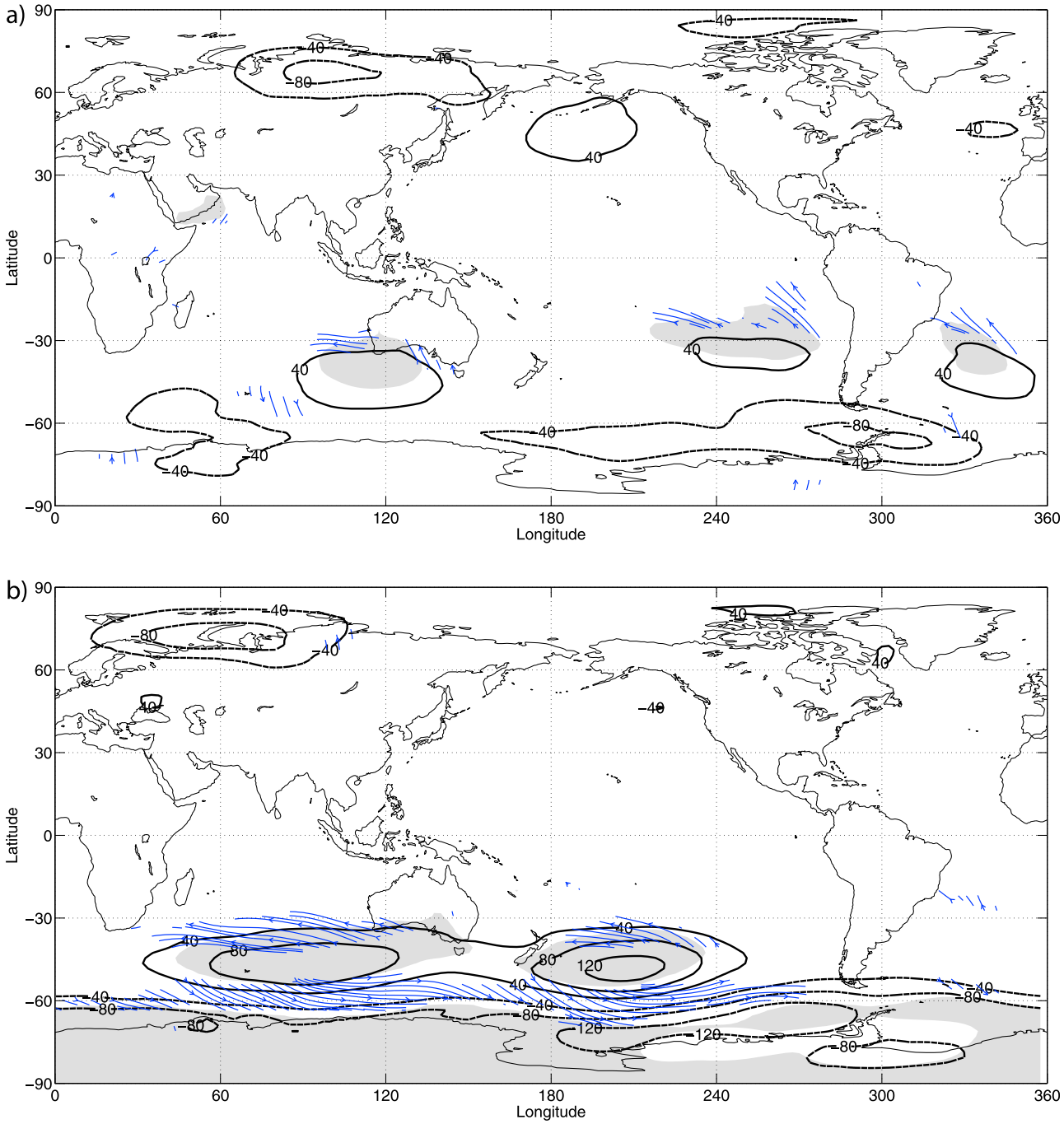

Figure 3. Same as Figure 2, but for atmospheric surface pressure in Pa for (a) A^{SC} and (b) A^{SC}_{QBO}. Arrows denote 99% significant wind anomalies. The maximum wind anomalies for Figure 3a reach $0.5\frac{m}{s}$ in the south Atlantic, while for Figure 3b, amplitudes of up to $0.9\frac{m}{s}$ occur around 60°S.

in the middle atmosphere can have a significant impact on the oceanic circulation.

4. Solar Signal in the Ocean Considering the QBO

[24] The analysis of the modeled oceanic reaction (O^{SC}) to the atmospheric forcing (A^{SC}) yields, as expected, a weak and non-significant response (not shown). We therefore focus our further analysis in this section on the ocean response (O^{SC}_{QBO}) to the more realistic atmospheric forcing, which includes the solar cycle and a nudged QBO (A^{SC}_{QBO}). We focus on the SH since the surface atmospheric forcing anomalies are strongest here (cf. Figure 3b). Figure 4a shows the solar cycle response of the ocean for the sea surface heights (SSH) and the oceanic surface currents. Shaded regions as well as streamlines show where the signal exceeds 99% statistical significance. Note that lagging the data does not enhance the signal. The shown oceanic surface current anomalies and SSH perturbations (Figure 4a) correspond

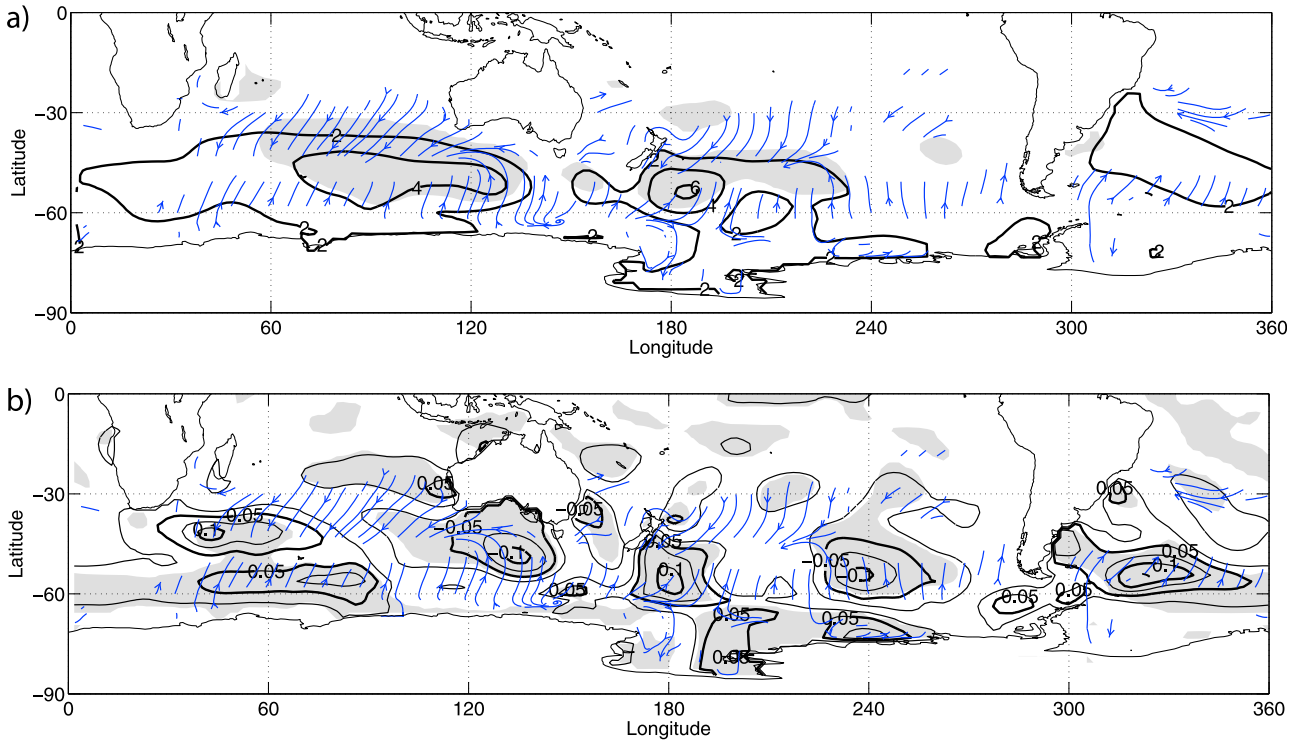

Figure 4. Annual mean composite mean difference between $S_{\max} - S_{\min}$ of (a) oceanic sea surface height (SSH) anomalies in cm and (b) sea surface temperature (SST) anomalies in K for O^{SC}_{QBO}. Arrows denote 99% significant current anomalies, with maximum amplitudes of $1.2\frac{cm}{s}$ in the southern Pacific.

well with the atmospheric surface forcing (Figure 3b). The maximum SSH response appears in the southern Indian and southern Pacific Ocean around 50°S. The corresponding current anomalies frame the SSH signal. The significant SSH anomalies vary between 2 and 6 cm, representing 20 to 45% of the local standard deviation of the monthly mean deseasonalized ocean data. On a decadal timescale we find significant surface atmospheric wind stress anomalies transferring momentum into the ocean (Figures 3b and 4). Due to the Coriolis force, wind-generated oceanic surface currents deviate toward the left in the SH. This deviation toward the left continues from ocean layer to ocean layer. The vertical integral gives the net effect of the mass transport, which is perpendicular to the original wind stress and thus points to the center of the positive surface pressure anomalies. Summarizing, we find the anticyclonic wind anomaly patterns (Figure 3b, experiment A^{SC}_{QBO}) inducing convergent oceanic surface currents (Figure 4a, experiment O^{SC}_{QBO}). This oceanic water convergence causes an increase in SSH at the center as well as a downwelling. Thus we find counter intuitive positive SSH anomalies in the regions of positive surface pressure anomalies (cf. Figures 3b and 4), which is the case during $S_{\max}$. *Boening et al.* [2011] found a similar phenomenon, though not related to the solar cycle, in the south east Pacific Ocean in November 2009 analyzing satellite altimetry and GRACE gravity field data. Here, an exceptionally persistent atmospheric high pressure field and the associated anticyclonic wind-forcing caused anomalous ocean currents, leading to oceanic convergence (positive SSH anomalies) toward the atmospheric high pressure field. This observation is in good agreement with our modeling results.

[25] In Figure 4b we show significant SST anomalies and the same oceanic surface current anomalies as in Figure 4a. We find a variety of significant positive and negative temperature anomalies, with an amplitude exceeding ±0.1 K. The significant temperature anomalies explain between 20 and 45% of the local standard deviation of the monthly mean deseasonalized ocean data. The shown anomalies cannot be attributed to atmospheric temperature anomalies and thus relate to a change in the oceanic surface state. In general we find positive temperature anomalies on the east side of the positive pressure anomalies and negative anomalies on the west side (cf. Figure 3b). This can be explained with the general anti-clockwise atmospheric wind anomalies and the associated ocean current anomalies. Both bring warmer water polewards on the east side and cooler water equatorwards on the west side. The question whether SST anomalies of a tenth of a K are sufficient to perturb the atmosphere significantly cannot be answered with our experiments and thus remains open for further studies.

5. Summary

[26] We used two atmospheric experiments from the chemistry-climate model WACCM, one with solar cycle only forcing (A^{SC}) and one with solar cycle and a nudged QBO (A^{SC}_{QBO}) to force the ocean general circulation model OMCT for 110 years. We first investigated the influence of the QBO on atmospheric near-surface conditions and found

a significant QBO signal in the surface pressure, which was accompanied by significant atmospheric surface wind field anomalies. However, this change in the atmospheric forcing did not translate into an oceanic response. This could be related to (1) the small magnitude of the perturbation and (2) the fast changing QBO signal (especially during short and strong easterly wind phases) to which the ocean cannot adjust that fast. We further investigated the effect of the QBO in combination with the solar cycle. We find that the presence of a QBO alters the solar cycle footprint in the northern stratosphere and strengthens it in the SH down to the surface (at around 50°S to 60°S), where positive zonal mean zonal wind anomalies reach the surface (Figure 2b) during $S_{\max}$. This agrees well with the findings of *Kuroda and Kodera* [2005], who found positive zonal mean zonal wind anomalies especially from October to December during $S_{\max}$. The results from the experiment with solar cycle and QBO (A^{SC}_{QBO}) deviate from the solar cycle only experiment (A^{SC}), where the solar cycle response is confined to the stratosphere only (Figure 2a). In the more realistic experiment with time-varying solar cycle and QBO (A^{SC}_{QBO}), we find, in agreement with *van Loon and Meehl* [2011], significant surface pressure anomalies, where positive SAM anomalies occur during $S_{\max}$ (Figure 3b). *Roy and Haigh* [2010] found similar but not statistically significant surface pressure anomalies. The associated atmospheric wind anomalies (Figure 3b) translate into oceanic surface current anomalies (Figure 4), which in the SH deviate left due to the Coriolis force. The transfer of momentum from the surface atmosphere to the surface ocean continues into deeper ocean layers (not explicitly shown). The net effect of the transport is perpendicular to the initial wind-forcing in the SH pointing toward the center of the positive surface pressure anomaly of an anticyclonic wind field (see Figure 3b). This leads to the convergence of ocean mass and the counter intuitive increase of SSHs in regions of positive surface pressure anomalies. According to *Wunsch and Stammer* [1997] one would expect that the ocean adjusts inverse barometrically such that the sea level rises in areas of low atmosphere pressure and falls in areas of high atmospheric pressure. However, we find an oceanic mass convergence, which is induced by an anticyclonic wind field. *Boening et al.* [2011] found a similar phenomenon in the south east Pacific Ocean in November 2009, where a persistent atmospheric high pressure field caused positive SSH anomalies.

[27] Furthermore, even though the presence of a QBO generally improves the atmospheric simulation, the nudging is also continuously perturbing an otherwise free-running model. As such, it prevents an atmospheric feedback into the nudging zone, for example via planetary waves. Nevertheless, a solar cycle signal at the surface atmosphere is only present in combination with a prescribed QBO. The question, whether this feature still occurs with an internally generated QBO, remains to be answered. However, we do find that changes in the middle atmosphere have the potential to influence the ocean surface and deeper layers on decadal timescale creating an integrated ocean mass convergence, which is visible as positive SSH anomalies. Taking this into account leads to the question, whether the perturbed ocean feeds back to the atmosphere, and whether this feedback enhances or mitigates the solar cycle footprint in the atmosphere. We assume that a possible feedback from the ocean into the atmosphere will not be induced by the shown SSH anomalies of a few cm (Figure 4). It is more likely that the atmospherically induced ocean current anomalies impact the atmosphere indirectly, by altering the SSTs. The here-shown SST anomalies of a tenth of K appear to be rather small, but they represent up to 40% of the standard deviation of the local monthly mean deseasonalized SSTs in our model. Due to the idealized character of our model study, the physical interpretation of this is limited. The scope of this analysis is to show that changes in the middle atmosphere effect the troposphere and even the ocean significantly, despite the small amplitudes. Consequently, comprehensive Earth System modeling studies should include models resolving the middle atmosphere (including the QBO) as well as a coupled ocean general circulation model.

6. Conclusions and Outlook

[28] Our experiments show that processes in the middle atmosphere (e.g. a transient prescribed QBO) can modulate the solar cycle response of the stratosphere. In our simulations we find that the insertion of the QBO significantly weakens the solar cycle response of the northern jet. Further we find a strengthening of the jet in the SH, which is significant only in the troposphere (Figure 2c). The extension of the solar cycle response of the southern jet from the stratosphere into the troposphere indicates increased stratosphere-troposphere coupling in the A^{SC}_{QBO} experiment. To summarize, the insertion of the QBO alters the "top-down" mechanism in the NH and it strengthens it in the SH, where we also find changes in the troposphere, which reach the surface (wind anomalies, Figure 3b). Finally these atmospheric surface wind anomalies alter the surface and deeper ocean dynamics as well as the SSHs. Moreover, we expect the oceanic reaction to feedback upon the atmosphere. We conclude: (1) The QBO influences the climate system response to the solar cycle in the atmosphere as well as in the ocean, especially in the SH. (2) This particularly strengthens the atmospheric "top-down" mechanism and brings the solar cycle response down to the surface. (3) In order to model a realistic climate response to varying natural forcings (e.g. solar cycle, QBO), numerical models need to include a realistically modeled middle atmosphere.

[29] We have shown that a realistic middle atmosphere is essential for modeling studies, that investigate the solar cycle response of the Earth system. We further showed an atmospherically induced solar cycle response of the ocean, which may have the potential to feed back to the atmosphere. However, the answer to this question remains for further studies.

[30] We plan to conduct these coupled Earth system experiments with NCAR's Community Earth System Model (CESM) in order to further quantify the natural variability of the climate system. Comparison of the coupled model output to the results shown here will allow the quantification of the atmosphere-ocean coupling effect.

[31] **Acknowledgments.** This work has been carried out within the Helmholtz-University Young Investigators Group NATHAN funded by the Helmholtz-Association through the President's Initiative and Networking Fund, the GFZ Potsdam, and by FU Berlin. The model calculations have been performed at the Deutsche Klimarechenzentrum (DKRZ) Hamburg. Furthermore, we wish to thank Lisa Neef, Felicitas Hansen, Julian Kuhlmann and three anonymous reviewers for constructive and helpful comments.

References

Boening, C., T. Lee, and V. Zlotnicki (2011), A record-high ocean bottom pressure in the South Pacific observed by GRACE, *Geophys. Res. Lett.*, *38*, L04602, doi:10.1029/2010GL046013.

Collins, W. D., et al. (2006), The Community Climate System Model Version 3 (CCSM3), *J. Clim.*, *19*(11), 2122–2143, doi:10.1175/JCLI3761.1.

Dobslaw, H., R. Dill, A. Grötzsch, A. Brzeziński, and M. Thomas (2010), Seasonal polar motion excitation from numerical models of atmosphere, ocean, and continental hydrosphere, *J. Geophys. Res.*, *115*, B10406, doi:10.1029/2009JB007127.

Drijfhout, S., C. Heinze, M. Latif, and E. Maier-Reimer (1996), Mean circulation and internal variability in an ocean primitive equation model, *J. Phys. Oceanogr.*, *26*(4), 559–580, doi:10.1175/1520-0485(1996)026<0559:MCAIVI>2.0.CO;2.

Flechtner, F. (2007), GFZ Level-2 processing standards document, technical report, GFZ Potsdam, Potsdam, Germany.

Garcia, R. R., D. R. Marsh, D. E. Kinnison, B. A. Boville, and F. Sassi (2007), Simulation of secular trends in the middle atmosphere, 1950–2003, *J. Geophys. Res.*, *112*, D09301, doi:10.1029/2006JD007485.

Gray, L. J., et al. (2010), Solar influences on climate, *Rev. Geophys.*, *48*, RG4001, doi:10.1029/2009RG000282.

Holton, J. R., and H.-C. Tan (1980), The influence of the equatorial quasi-biennial oscillation on the global circulation at 50 mb, *J. Atmos. Sci.*, *37*(10), 2200–2208, doi:10.1175/1520-0469(1980)037<2200:TIOTEQ>2.0.CO;2.

Holton, J. R., and H.-C. Tan (1982), The quasi-biennial oscillation in the Northern Hemisphere lower stratosphere, *J. Meteorol. Soc. Jpn.*, *60*, 140–148.

Huang, B., and V. M. Mehta (2005), Response of the Pacific and Atlantic oceans to interannual variations in net atmospheric freshwater, *J. Geophys. Res.*, *110*, C08008, doi:10.1029/2004JC002830.

Kinnison, D. E. (2007), Sensitivity of chemical tracers to meteorological parameters in the MOZART-3 chemical transport model, *J. Geophys. Res.*, *112*, D20302, doi:10.1029/2006JD007879.

Kodera, K., and Y. Kuroda (2002), Dynamical response to the solar cycle, *J. Geophys. Res.*, *107*(D24), 4749, doi:10.1029/2002JD002224.

Kuroda, Y., and K. Kodera (2005), Solar cycle modulation of the Southern Annular Mode, *Geophys. Res. Lett.*, *32*, L13802, doi:10.1029/2005GL022516.

Labitzke, K. (1987), Sunspots, the QBO, and the stratospheric temperature in the north polar region, *Geophys. Res. Lett.*, *14*(5), 535–537, doi:10.1029/GL014i005p00535.

Labitzke, K., and H. V. Loon (1988), Associations between the 11-year solar cycle, the QBO and the atmosphere. Part I: The troposphere and stratosphere in the Northern Hemisphere in winter, *J. Atmos. Terr. Phys.*, *50*(3), 197–206.

Marsh, D. R., and R. R. Garcia (2007), Attribution of decadal variability in lower-stratospheric tropical ozone, *Geophys. Res. Lett.*, *34*, L21807, doi:10.1029/2007GL030935.

Matthes, K., D. R. Marsh, R. R. Garcia, D. E. Kinnison, F. Sassi, and S. Walters (2010), Role of the QBO in modulating the influence of the 11 year solar cycle on the atmosphere using constant forcings, *J. Geophys. Res.*, *115*, D18110, doi:10.1029/2009JD013020.

Meehl, G. A., J. M. Arblaster, K. Matthes, F. Sassi, and H. van Loon (2009), Amplifying the Pacific climate system response to a small 11-year solar cycle forcing, *Science*, *325*(5944), 1114–1118, doi:10.1126/science.1172872.

Rind, D., J. Lean, J. Lerner, P. Lonergan, and A. Leboissitier (2008), Exploring the stratospheric/tropospheric response to solar forcing, *J. Geophys. Res.*, *113*, D24103, doi:10.1029/2008JD010114.

Roy, I., and J. D. Haigh (2010), Solar cycle signals in sea level pressure and sea surface temperature, *Atmos. Chem. Phys.*, *10*(6), 3147–3153, doi:10.5194/acp-10-3147-2010.

Thomas, M., J. Sündermann, and E. Maier-Reimer (2001), Consideration of ocean tides in an OGCM and impacts on subseasonal to decadal polar motion excitation, *Geophys. Res. Lett.*, *28*(12), 2457–2460.

Thompson, D. W. J., and J. M. Wallace (2000), Annular modes in the extratropical circulation. Part I: Month-to-month variability, *J. Clim.*, *13*(5), 1000–1016, doi:10.1175/1520-0442(2000)013<1000:AMITEC>2.0.CO;2.

van Loon, H., and G. A. Meehl (2011), The average influence of decadal solar forcing on the atmosphere in the South Pacific region, *Geophys. Res. Lett.*, *38*, L12804, doi:10.1029/2011GL047794.

White, W. B., J. Lean, D. R. Cayan, and M. D. Dettinger (1997), Response of global upper ocean temperature to changing solar irradiance, *J. Geophys. Res.*, *102*(C2), 3255–3266.

Wolff, J.-O., E. Maier-Reimer, and S. Legutke (1996), The Hamburg Ocean Primitive Equation Model HOPE, *Tech. Rep.*, *13*, 103 pp., German Clim. Comput. Cent., Hamburg, Germany.

Wunsch, C., and D. Stammer (1997), Atmospheric loading and the oceanic "inverted barometer" effect, *Rev. Geophys.*, *35*(1), 79–107, doi:10.1029/96RG03037.